5-1-2011

Transforming the Fabrication and Biofunctionalization of Gold Nanoelectrode Arrays into Versatile Electrochemical Glucose Biosensors

Jonathan C. Claussen
Bindley Bioscience Center, Purdue University, jclausse@purdue.edu

Monique Wickner
Purdue University

Timothy S. Fisher
Birck Nanotechnology Center, Purdue University, tsfisher@purdue.edu

D. Marshall Porterfield
Birck Nanotechnology Center, Purdue University, porterf@purdue.edu

ACS APPLIED MATERIALS & INTERFACES

RESEARCH ARTICLE

www.acsami.org

Transforming the Fabrication and Biofunctionalization of Gold Nanoelectrode Arrays into Versatile Electrochemical Glucose Biosensors

Jonathan C. Claussen,[†,‡,§] Monique M. Wickner,[†,§] Timothy S. Fisher,[†,⊥] and D. Marshall Porterfield[*,†,‡,§,∥]

[†]Birck Nanotechnology Center, West Lafayette, Indiana 47907, United States

[‡]Bindley Bioscience Center—Physiological Sensing Facility, West Lafayette, Indiana 47907, United States

[§]Department of Agricultural and Biological Engineering, West Lafayette, Indiana 47907, United States

[⊥]School of Mechanical Engineering, West Lafayette, Indiana 47907, United States

[∥]Weldon School of Biomedical Engineering, West Lafayette, Indiana 47907, United States

ABSTRACT: High-density arrays of conducting nanoelectrodes (i.e., nanoelectrode arrays [NEAs]) have been developed on the surface of a single electrode for numerous electrochemical sensing paradigms. However, a scalable fabrication technique and robust biofunctionalization protocol are oftentimes lacking and thus many NEA designs have limited efficacy and overall commercial viability in biosensing applications. In this report, we develop a lithography-free nanofabrication protocol to create large arrays of Au nanoelectrodes on a silicon wafer via a porous anodic alumina template. To demonstrate their effectiveness as electrochemical glucose biosensors, alkanethiol self-assembled monolayers (SAMs) are used to covalently attach the enzyme glucose oxidase to the Au NEA surface for subsequent glucose sensing. The sensitivity and linear sensing range of the biosensor is controlled by introducing higher concentrations of long-chain SAMs (11-mercaptoundecanoic acid: MUA) with short-chain SAMs (3-mercaptopropionic acid: MPA) into the enzyme immobilization scheme. This facile NEA fabrication protocol (that is well-suited for integration into electronic devices) and biosensor performance controllability (via the mixed-length enzyme-conjugated SAMs) transforms the Au NEAs into versatile glucose biosensors. Thus these Au NEAs could potentially be used in important real-word applications such as in health-care and bioenergy where biosensors with very distinct sensing capabilities are needed.

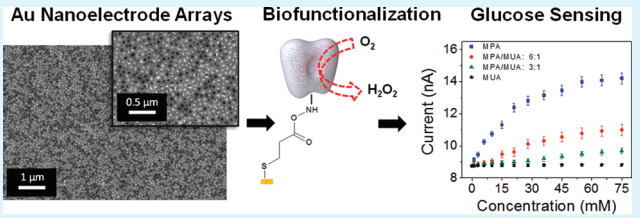

KEYWORDS: nanoelectrode arrays, self-assembled monolayers, glucose biosensor, glucose oxidase, porous anodic alumina

INTRODUCTION

Recent developments in nanotechnology have provoked the creation of miniature electrochemical electrodes with nanoscale dimensions (1−100 nm).[1−3] Fundamental electrochemical research has elucidated their unique properties including higher current densities, more favorable Faradic-to-capacitive current ratios, and faster mass transport by convergent (radial) diffusion than macro-/microelectrodes.[4−7] These properties have improved electrode performance including faster response times, lower detection limits, and improved mass transport kinetics. To increase their measurable current signal and expand their efficacy in biosensing applications, high-density arrays of conducting nanoelectrodes (i.e., nanoelectrode arrays [NEAs]) separated by nonconducting oxide material have been developed on the surface of a single electrode.[8−12] These NEA sensors, fabricated in various geometries (e.g., nanopores, nanobands, and nanodisks) have shown promising results, displaying high sensitivities and fast response times; however, a scalable fabrication technique and robust biofunctionalization protocol are oftentimes lacking.

In order to advance the emerging technology of NEAs into commercially viable biosensing applications, fundamental fabrication challenges still need to be addressed. For example, many NEA designs require lithographic and chemical processing steps that are often expensive, limited to serial processing, and not suitable for a wide variety of materials.[13] Thus many NEA fabrication schemes are not compatible with the high-throughput/low cost electrode design necessary for medical devices, such as blood glucose monitors.[14,15] However, templated growth of nanoelectrodes offers a promising solution as they are relatively inexpensive, adaptable to numerous materials and substrates, and allow for facile patterning of large surface areas. NEAs of various shapes and sizes have been fabricated by electrodepositing noble metals into the nanosized pores of polycarbonate (PC)[16−18] and porous anodic alumina (PAA)[19−21] templates. PC templates contain carbonyl groups that can react with proteins and thus are susceptible to fouling during in vitro or in vivo experimentation.[22,23] However, PAA templates are biochemically inert and display material characteristics (e.g., uniform pore size, high pore density, hardness, preparation ease) that are well-suited for high throughput manufacturing and biological applications.[24]

Received: March 9, 2011
Accepted: April 25, 2011
Published: April 25, 2011

The successful application of nanoelectrode arrays to commercial biosensors also depends heavily on the ability to robustly attach biorecognition agents (e.g., enzymes, antibodies, and DNA) to nanoscale electrode surfaces. Attachment techniques that utilize polymers such as nafion,[25] chitosan,[26] and silicate sol gels[27] generally coat the entire electrode surface—thus creating an additional diffusion layer that can impede mass transport of target analyte and potentially negate the effects of radial diffusion. Furthermore, noncovalent membrane based immobilization techniques are subject to delamination and show limited reproducibility in biological sensing applications.[28] However, self-assembled monolayers (SAMs) offer a robust and versatile molecular immobilization strategy for biosensors.[29] SAMs form strong Au−S covalent bonds that can be chemically modified to link with a wide variety of biological systems.[30,31] Thus SAMs provide a strong and stable attachment mechanism for immobilizing biorecognition agents close to the electrode surface—facilitating diffusion of target analyte and decreasing the distance for electron transfer.

Several groups have shown the ability to amperometrically detect glucose by tethering the enzyme GOx to Au macro and microbiosensors with short-chain and long-chain SAMs, including 3-mercaptopronionic acid (MPA), 11-mercapoundecanoic acid (MUA), and *N*-hydroxysuccinimide (NHS) modified 16-mercaptohexadecanoic (MHA).[28,32−35] Though SAMs have proven effective in immobilizing active enzyme close to the electrode surface for biosensing purposes, they have also shown to insulate the surface of the electrode—impeding heterogeneous charge transport at the electrode/liquid interface and consequently reducing biosensor sensitivity. These electrical insulating effects can potentially negate the current response received from nanoelectrode arrays where size constraints already greatly reduce the surface area for electron transport and enzyme immobilization. Thus, in this work, we aim to examine the effects of both short- and long-chain enzyme-conjugated SAMs immobilized on NEAs in an effort to control the performance of the biosensor (i.e., sensitivity, linear sensing range, and detection limit) by manipulating the length and composition of the immobilized SAM structure.

Herein, we present a facile bottom-up approach to creating glucose biosensors by fabricating arrays of Au nanoelectrodes from a silicon chip templated with PAA. We electrochemically characterize the Au NEAs and analyze their sensitivity to hydrogen peroxide (H_2O_2), the measurable electroactive product of the GOx/glucose reaction, when functionalized with short-chain (MPA) and long-chain (MUA) SAMs. We transform the Au NEAs into glucose biosensors by immobilizing GOx-conjugated SAMs on the biosensor surface. The biosensor performance is controlled by manipulating the length and composition of the immobilized SAM structure. GOx-conjugated SAMs comprised of MPA, MUA, and mixed-length SAMs (MPA/MUA 6:1 and MPA/MUA 3:1) are all immobilized on the Au NEAs and subsequently tested.

MATERIALS AND METHODS

Au Nanoelectrode Array (NEA) Template. A porous anodic alumina (PAA) substrate is utilized as a template to create the arrays of Au nanoelectrodes. Similar to our previous work,[36−38] the PAA template is created by first e-beam evaporating (base pressure: 5.0×10^{-7} Torr) a thin film metal stack of Ti (100 nm) and then Al (300 nm) onto an oxidized silicon wafer [*P* <100> Si (5 μm), SiO_2 (500 nm)]. Subsequently the Al layer is transformed into alumina through an anodization technique that involves biasing the metalized wafer sample with 40 V versus a Pt gauze auxiliary electrode within a 0.3 M oxalic acid bath held at 1.5 °C. This anodization process converts the Al into the dielectric Al_2O_3 and creates semiordered pores approximately 20 nm in diameter that extends through the Al_2O_3 to the Ti layer. An electrical contact pad for subsequent electrical integration with electrochemical sensing equipment is created by leaving a portion of the sample unanodized. In this setup, the Ti bottom layer provides electrical contact between the contact pad and the base of the Au nanowires deposited within the pores of the PAA.

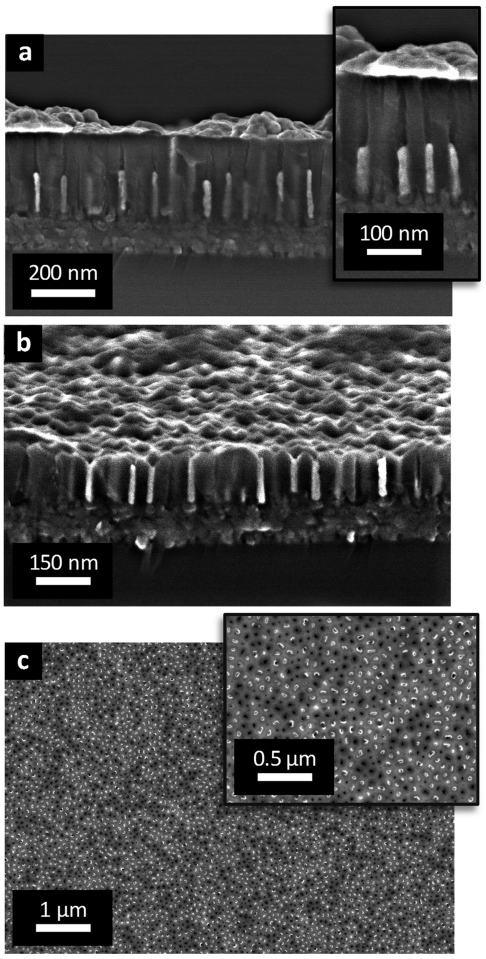

Figure 1. Field emission scanning electron microscopy (FESEM) micrographs illustrating the fabrication of the Au nanoelectrode arrays (NEAs). Side-view micrographs portraying (a) Au nanorods (150 nm in length) electrodeposited into the PAA template with inset showing a magnified view and (b) the exposed tips of the nanorods after Ar ion milling. (c) Top-view micrograph portraying the Au nanoelectrode arrays with inset showing a magnified view.

Au Electrodeposition and NEA Formation. The Au NEAs are formed by electrodepositing Au into the 20 nm pores of the PAA. First, the innate oxide barrier at the base of the pores is penetrated by exposing the sample to a high-temperature hydrogen plasma within a SEKI AX5200S microwave plasma chemical vapor deposition (MPCVD) reactor. The sample is heated to 900 °C within a hydrogen ambient by a 3.5 kW radio frequency power supply on a 5.1 cm diameter molybdenum puck. After a 10 min exposure to the high-temperature plasma, Au is electrodeposited into the pores of the PAA by immersing the sample into an Au(III) chloride hydrate solution (Sigma Aldrich: 254169). The electrodeposition of Au is carried out by a three-electrode

setup (BASi Epsilon Cell Stand) where the exposed Ti layer at the base of the pores act as the working electrode, Pt gauze, as the auxiliary electrode, and Ag/AgCl as the reference electrode. Pulsed electrical currents of 10 mA/cm^2 are applied between the working and auxiliary electrodes at a frequency of 500 ms to create Au nanorods approximately 150 nm in length within the pores of the PAA (Figure 1a). Argon ion bombardment within a Panasonic E620 dry etching system is utilized to mill back the PAA to expose the tips of the nanorods, creating arrays of Au nanoelectrodes separated by oxide (Figure 1b and c).

Alkanethiol Self-Assembled Monolayer (SAM) Formation. In order to clean the electrode surface prior to self-assembled monolayer (SAM) formation and to remove SAM layers after formation, the Au NEA was electrochemically cleaned with 0.3 M H_2SO_4 by cycling the potential from −500 to 1500 mV at a scan rate of 100 mV/s. Theses cleaning cycles were repeated approximately 20 times or until the shape of the voltammograms became immutable. The electrode was then solvent cleaned and dried under a gentle stream of nitrogen gas. SAM layers consisting of 3-mercaptopropionic acid (MPA), 11-mercaptoundecanoic acid (MUA), and a mixed ratio of MPA/MUA, 6:1 and 3:1 respectively, were immobilized according to similar protocols.[34] The three distinct SAM cocktails are created by dissolving 40 mM MPA, 40 mM MUA, and 40 mM MPA/MUA in a 6:1 or a 3:1 ratio in ethanol/H_2O (75%/25%) solution in separate test vials. The Au NEA was immersed and soaked in a single test vial for 15 h (MPA and MUA) or 3 h (MPA/MUA), respectively, at room temperature. After eventual enzyme conjugation and electrochemical sensing, the electrode was again electrochemically cleaned with 0.3 M H_2SO_4 and functionalized with the subsequent SAM layer according to the same protocol mentioned beforehand.

Glucose Oxidase (GOx) Enzyme Immobilization. After each distinct SAM was formed, the electrode was rinsed with ethanol and ultrapure water. The carboxyl group located on the free end of each thiol linker was activated by immersing the electrode in a 0.1 M 2-(*N*-morpholino) ethanesulfonic acid (MES) [Sigma Aldrich: M3671] acid with 15 mM *N*-hydroxysuccinimide (NHS) [Sigma Aldrich: 130672] and 75 mM 1-[3-(dimethylamino)propyl]-3-ethylcarbodiimide methiodide (EDC) [Sigma Aldrich: 165344] for 2 h. After the carboxyl group was activated, the electrode was rinsed thrice with 0.1 M phosphate buffered saline (PBS: pH = 7.4) and immersed in the enzyme solution containing 0.1 M PBS with 2 mg/mL glucose oxidase (GOx) [Sigma Aldrich: G7141]. In order to promote enzyme immobilization, the electrode/enzyme solution was gently agitated for 2 h in a test tube shaker. To prevent enzyme denaturing, the electrode was stored in 0.1 M PBS at 4 °C until electrochemical testing.

Electrochemical Sensing. A three-electrode electrochemical setup (BASi Epsilon Three-Electrode Cell Stand), as used in the Au electrodeposition, was utilized for all amperometric experiments. The respective Au NEAs biosensors act as the working electrode, Ag/AgCl as the reference electrode, and a Pt wire as the auxiliary electrode. Amperometric measurements were performed in phosphate buffered saline (PBS, 0.1 M pH 7.4) at an overvoltage of 500 mV. During H_2O_2 and glucose sensing, successive increasing concentration aliquots of said target analyte are injected into the test vial while the solution is continuously stirred (500 rpm) with a 0.5 cm (length) magnetic stir bar. The Ti bottom layer that electrically contacts the Au nanowires at the base of the PAA pores is electrically wired to the potentiostat (BASi Epsilon Three-Electrode Cell Stand). Electrons generated at the surface of the Au NEAs flow to the cell stand via the nanowires and conductive Ti underlayer.

Imaging. A S-4800 Hitachi microscope was utilized at a power setting of 5.0 kV to obtain the field emission scanning electron microscopy (FESEM) micrographs. Samples were imaged before immobilization of GOx enzyme without any additional processing steps.

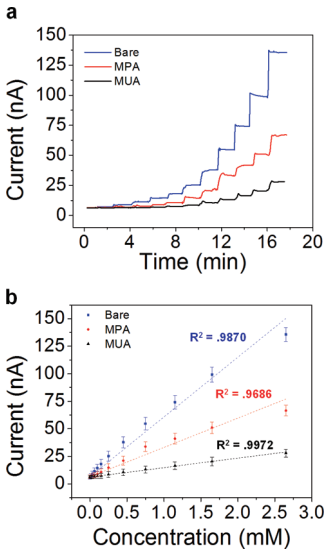

Figure 2. H_2O_2 calibration plot carried out in 20 mL of PBS (pH 7.4) at an applied working potential of 500 mV for the Au NEA (bare (blue), functionalized with MPA (red), and functionalized with MUA (black)). (a) Calibration plot illustrating the dynamic current response for successive H_2O_2 concentration increases of 20−50 μM by 10 μM, 100−500 μM by 100 μM, and finally a 1 mM aliquot. (b) Current versus concentration plot with dotted dash lines showing linear regression analysis of the current vs concentration profiles with the corresponding coefficient of determination (R^2). Error bars show standard deviation for three different experiments.

RESULTS AND DISCUSSION

Amperometric H_2O_2 Sensing. In order to test the capability of the sensor to act as a biosensor, H_2O_2 calibration plots were performed. H_2O_2 is important to glucose sensing, because it is the measurable electroactive species produced from the enzymatic breakdown of glucose via the enzyme glucose oxidase (GOx). The production of H_2O_2 from the GOx/glucose reaction and the subsequent oxidation of H_2O_2 at the electrode surface is portrayed in eqs 1 and 2.

$$\text{D-glucose} + O_2 + H_2O \xrightarrow{\text{GOx}} \text{D-gluconic acid} + H_2O_2 \quad (1)$$

$$H_2O_2 \rightarrow 2H^+ + O_2 + 2e^- \quad (2)$$

The effects of both short-chain and long-chain SAMs on H_2O_2 sensitivity is monitored by comparing the current response to bare Au NEAs and those immobilized with both MPA and MUA. Successive increasing concentration aliquots of H_2O_2 are injected into the test vial containing buffered phosphate saline (PBS: pH 7.4) while the solution is continuously stirred (500 rpm) (Figure 2). The immobilization of short-chain (MPA) and long-chain (MUA) on the Au NEA sensor considerably reduces the sensitivity to H_2O_2. These results confirm previous reports that conclude that long-chain alkanethiols form more densely and accordingly create a greater electron-transfer barrier on gold surfaces than short-chain alkanethiol SAMs.[33,34,39] Thus, in the case of H_2O_2 oxidation, the short-chain alkanethiol (MPA) reduces the sensitivity of the Au NEAs by more than a factor of 2 from 144 to 69.2 nA mM^{-1} cm^{-2} while the long-chain alkanethiol (MUA) almost completely impedes heterogeneous

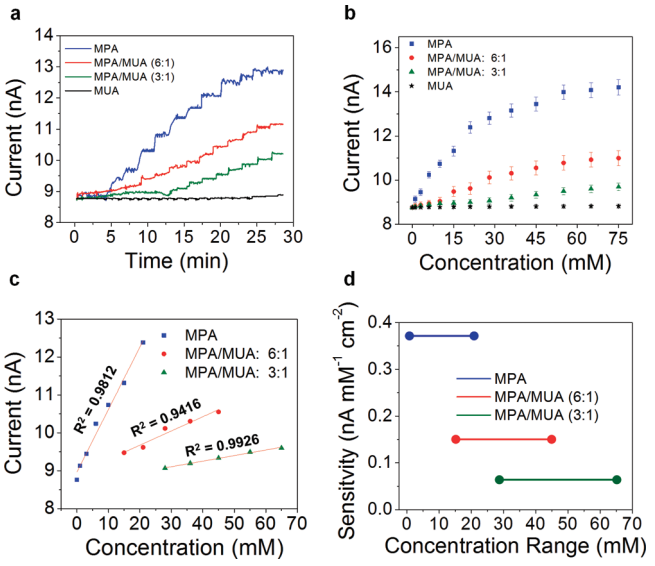

Figure 3. Amperometric glucose sensing calibration plots in 20 mL of PBS (pH 7.4) at an applied working potential of 500 mV for the Au nanoelectrode array electrode functionalized with enzyme conjugated MPA (blue), MPA/MUA (6:1; red), MPA/MUA (3:1; green), and MUA (black). (a) Calibration plot illustrating the dynamic current response for successive glucose concentration increases of 1−10 mM by 1 mM followed by two 10 mM aliquots and (b) corresponding current vs concentration glucose concentration plot where error bars show standard deviation for three different experiments. (c) Linear glucose sensing range with linear regression analysis of the current vs concentration profiles showing the corresponding coefficient of determination (R^2) and (d) graphical representation of the sensitivity vs linear glucose sensing range.

charge transport by reducing the H_2O_2 sensitivity to 23.9 nA mM^{-1} cm^{-2} (Figure 2).

Amperometric Glucose Sensing. Amperometric glucose sensing is realized by immobilizing the active GOx enzyme on the Au NEAs surfaces through carbodimmide chemistry (see Materials and Methods). In an effort to more closely monitor the effects of enzyme conjugated SAM layer density on glucose sensitivity, the Au NEAs were functionalized with both MPA and MUA SAM layers as well as mixed layer SAMs (MPA/MUA 6:1 and MPA/MUA 3:1). Amperometric glucose sensing was performed under the same working potential and 3-electrode setup as the H_2O_2 sensing. Successive increasing concentration aliquots of glucose are injected into the test vial while the solution is continuously stirred (500 rpm). The amperometric glucose calibration plot, current vs concentration profiles, and sensitivity vs linear sensing range plot for the GOx-SAM functionalized Au NEAs are all displayed in Figure 3.

Similar to the amperometric H_2O_2 results, the Au NEA biosensor functionalized with MPA displayed the highest sensitivity to glucose—substantially distancing itself from the sensitivity of the mixed length GOx-SAM functionalized sensors (Figure 3d). This observed glucose sensitivity gap between the MPA functionalized electrodes and mixed-length (MPA/MUA) functionalized electrodes follows similar observations made by Whitesides and co-workers in which the formation of longer chain thiols is favored over shorter chain thiols in mixed-length SAM reactions.[40] Thus even with a high ratio of short-chain MPA to long-chain MUA in the mixed

Table 1. Amperometric Glucose Sensing Performance Comparison of Au-Based Electrodes Including Glucose Biosensors Based upon Macrodisks, Microdisks, and Nanoelectrode Arrays[a]

biosensor	detection limit (mM)	linear sensing range (mM)	ref
GOx-MPA-Au NEA-PAA	0.1	1−21	this work
GOx-MPA/MUA (6:1)-Au NEA-PAA	3.1	15−45	this work
GOx-MPA/MUA (3:1)-Au NEA-PAA	12.4	28−65	this work
GOx-NHS-MHA-Au-UME	0.06	1−5	28
TTF-GOx-MPA-AuDE	0.0035	1−6	33
GOx-BSA-Au NEA	0.005	0.01−10	41
Au NWEA-PDMS-Glass	0.05	1−10	42
GOx/Au_{coll}-Cyst-AuDE	0.0067	0.01−10	43
GOx-HRP-GA-MPA-AuNEA-PC	0.1	up to 17	44
porous Au film	0.05	2−10	45

[a] Abbreviations: (GOx) glucose oxidase, (MPA) 3-mercaptopronionic acid, (MUA) 11-mercaptoundecanoic acid (Au) gold, (NEA) nanoelectrode array, (NHS) *N*-hydroxysuccinimide, (MHA) 16-mercaptohexadecanoic acid, (PAA) porous anodic alumina, (UME) ultramicroelectrode, (TTF) tetrathiafulvalene, (AuDE) Au disk electrode, (BSA) bovine serum albumin, (NWEA) nanowire electrode array, (PDMS) poly(dimethylsiloxane), (Aucoll) colloidal gold, (Cyst) cysteamine, (HRP) horseradish peroxidase, (GA) glutaraldehyde, (PC) polycarbonate.

length SAM immobilization protocol, as in the case of MPA/MUA (6:1), the long-chain MUA preferentially forms over the short chain MPA on the biosensor surface—establishing a denser and more electrically insulating SAM structure on the Au NEAs. Therefore, the addition of MUA in the MPA/MUA (6:1) GOx-conjugated SAM biosensor substantially reduces the glucose sensitivity by more than a factor of 4 from 0.47 to 0.11 nA mM^{-1} cm^{-2}. The higher ratio of MUA in the MPA/MUA (3:1) GOx-conjugated SAM biosensor further reduces the glucose sensitivity to 0.04 nA mM^{-1} cm^{-2}, while the sensitivity of the MUA functionalized biosensor is negligible. The glucose linear sensing range and detection limit (based upon a signal-to-noise ratio of 3) for the MPA, MPA/MUA (6:1), and MPA/MUA (3:1) GOx-conjugated Au NEA glucose biosensors are compared to the performance of typical Au-based macrodisks, microdisks, and nanoelectrode arrays presented in the literature (Table 1).

These amperometric glucose sensing results (Table 1) confirm that the linear sensing range and detection limit of the Au NEA glucose biosensors can be adjusted by manipulating the length and composition of the enzyme-conjugated SAMs. As the biosensor sensitivity decreases, the detection limit decreases, and the linear sensing regions shift to higher concentrations. This ability to control the detection limit and linear sensing regions of electrochemical biosensors is important to many biological and physiological sensing applications. In the glucose sensing paradigm, for example, the Au NEA biosensors functionalized with GOx via MPA could potentially be used to monitor blood glucose levels where the physiological range for blood glucose is typically between 3.6 and 7.5 mM (65−135 mg/dL) for healthy patients and

between 1.1 and 19.4 mM (20−350 mg/dL) for diabetic patients. Thus these Au NEAs improve upon the linear range reported for many Au macrodisk, microdisk, and similar nanoelectrode array glucose biosensors (Table 1) and open the door for integration into devices for glucose monitoring in both healthy and diabetic patients. Furthermore, the Au NEAs functionalized with MPA/MUA (6:1) and MPA/MUA (3:1) could be utilized in some large scale bioreactors where critical glucose feeding concentrations can vary from 20 to 50 mM, respectively.[46,47]

CONCLUSIONS

We developed a facile nanofabrication protocol for creating large arrays of Au nanoelectrodes fabricated on a silicon chip. We fabricate these Au NEAs by utilizing a bottom-up approach to develop a porous anodic alumina (PAA) template on a silicon chip and by subsequently electrodepositing Au into the pores of the PAA. A top-down approach to etchback the PAA was used to expose the Au NEAs for subsequent biofunctionalization and electrochemical biosensing. The sensitivity to glucose is controlled by manipulating the length and composition of the immobilized GOx-conjugated SAMs. This controllable shift in glucose sensitivity and likewise linear sensing range allows biosensor development for specific applications. Thus these Au NEAs prove to be quite versatile and could potentially be developed to sense concentration levels that are targeted for unique applications such as glucose monitoring in blood and bioreactors.

In summary, the performance of the presented Au NEA biosensors can be controlled for distinct biosensing applications with potential scalability for use in commercial applications. This unique nanofabrication protocol and side-by-side comparison study of immobilized variable-length enzyme-conjugated SAMs is fundamental for the transformation of NEAs into real-world commercial biosensors. Thus, this research serves as a stepping stone for future work were the Au NEA biosensor design protocol can be adjusted for specific biological and physiological sensing requirements—including packaging and dimensional modifications as well as the inclusion of anion-repellents to minimize the effects of electrochemical interference from electroactive, endogenous species.

AUTHOR INFORMATION

Corresponding Author

*Mailing address: Purdue University Department of Agricultural and Biological Engineering, 225 South University Street, West Lafayette, IN 47907-2093 Office ABE 319. Phone: (765) 494-1190. Fax: (765) 496-1115. E-mail: porterf@purdue.edu.

ACKNOWLEDGMENT

The authors would like to gratefully acknowledge assistance from the Purdue Physiological Sensing Facility and Purdue Nanoscale Transport Research Group of the Birck Nanotechnology Center and Bindley Bioscience Center. We graciously recognize funding support from the Office of Naval Research, National Science Foundation, and the Purdue Research Foundation Trask Fund. A special thanks is also extended to Michel Schweinsberg for assistance in figure creation.

REFERENCES

(1) Alivisatos, P. *Nat. Biotechnol.* **2004**, *22*, 47.
(2) Drummond, T. G.; Hill, M. G.; Barton, J. K. *Nat. Biotechnol.* **2003**, *21*, 1192.
(3) Murray, R. W. *Chem. Rev.* **2008**, *108*, 2688.
(4) Arrigan, D. W. M. *Analyst* **2004**, *129*, 1157.
(5) Compton, R. G.; Wildgoose, G. G.; Rees, N. V.; Streeter, I.; Baron, R. *Chem. Phys. Lett.* **2008**, *459*, 1.
(6) Jena, B. K.; Percival, S. J.; Zhang, B. *Anal. Chem.* **2010**, 1041.
(7) Li, Y.; Cox, J. T.; Zhang, B. *J. Am. Chem. Soc.* **2010**, *132*, 3047.
(8) Ito, T.; Audi, A. A.; Dible, G. P. *Anal. Chem.* **2006**, *78*, 7048.
(9) Lanyon, Y. H.; Arrigan, D. W. M. *Sens. Actuators, B* **2007**, *121*, 341.
(10) Le Saux, G.; Ciampi, S.; Gaus, K.; Gooding, J. J. *ACS Appl. Mater. Interfaces* **2009**, *1*, 2477.
(11) Lupu, A.; Lisboa, P.; Valsesia, A.; Colpo, P.; Rossi, F. *Sens. Actuators, B* **2009**, *137*, 56.
(12) Sandison, M. E.; Cooper, J. M. *Lab Chip* **2006**, *6*, 1020.
(13) Sander, M. S.; Tan, L. S. *Adv. Funct. Mater.* **2003**, *13*, 393.
(14) Luong, J. H. T.; Male, K. B.; Glennon, J. D. *Biotechnol. Adv* **2008**, *26*, 492.
(15) Newman, J. D.; Turner, A. P. F. *Biosens. Bioelectron.* **2005**, *20*, 2435.
(16) De Leo, M.; Kuhn, A.; Ugo, P. *Electroanalysis* **2007**, *19*, 227.
(17) Menon, V. P.; Martin, C. R. *Anal. Chem.* **1995**, *67*, 1920.
(18) Perera, D. M. N. T.; Ito, T. *Analyst* **2009**, *135*, 172.
(19) Borissov, D.; Isik-Uppenkamp, S.; Rohwerder, M. *J. Phys. Chem. C* **2009**, *113*, 3133.
(20) Shin, C.; Shin, W.; Hong, H. G. *Electrochim. Acta* **2007**, *53*, 720.
(21) Tan, L. K.; Chong, A. S. M.; Tang, X. S. E.; Gao, H. *J. Phys. Chem. C* **2007**, *111*, 4964.
(22) Mucelli, S. P.; Zamuner, M.; Tormen, M.; Stanta, G.; Ugo, P. *Biosens. Bioelectron.* **2008**, *23*, 1900.
(23) Rucker, V. C.; Havenstrite, K. L.; Simmons, B. A.; Sickafoose, S. M.; Herr, A. E; Shediac, R. e *Langmuir* **2005**, *21*, 7621.
(24) Piao, Y.; Kim, H. *J. Nanosci. Nanotechnol.* **2009**, *9*, 2215.
(25) Karyakin, A. A.; Gitelmacher, O. V.; Karyakina, E. E. *Anal. Chem.* **1995**, *67*, 2419.
(26) Kang, X.; Mai, Z.; Zou, X.; Cai, P.; Mo, J. *Anal. Biochem.* **2007**, *369*, 71.
(27) Chen, H.; Dong, S. *Biosens. Bioelectron.* **2007**, *22*, 1811.
(28) Masson, J. F.; Kranz, C.; Booksh, K. S.; Mizaikoff, B. *Biosens. Bioelectron.* **2007**, *23*, 355.
(29) Chaki, N. K.; Vijayamohanan, K. *Biosens. Bioelectron.* **2002**, *17*, 1.
(30) Evans, S. D.; Ulman, A. *Chem. Phys. Lett.* **1990**, *170*, 462.
(31) Love, J. C.; Estroff, L. A.; Kriebel, J. K.; Nuzzo, R. G.; Whitesides, G. M. *Chem. Rev.* **2005**, *105*, 1103.
(32) Anandan, V.; Gangadharan, R.; Zhang, G. *Sensors* **2009**, *9*, 1295.
(33) Campuzano, S.; Gálvez, R.; Pedrero, M.; de Villena, F.; Pingarrón, J. M. *J. Electroanal. Chem.* **2002**, *526*, 92.
(34) Campuzano, S.; Pedrero, M.; Montemayor, C.; Fatás, E.; Pingarrón, J. M. *J. Electroanal. Chem.* **2006**, *586*, 112.
(35) Gooding, J. J.; Hibbert, D. B. *TrAC Trends Anal. Chem.* **1999**, *18*, 525.
(36) Claussen, J. C.; Franklin, A. D.; ul Haque, A.; Porterfield, D. M.; Fisher, T. S. *ACS Nano* **2009**, *3*, 37.
(37) Claussen, J. C.; Sungwon, K. S.; Haque, A. u.; Artiles, M. S.; Porterfield, D. M.; Fisher, T. S. *J. Diabetes Sci. Technol.* **2010**, *4*, 312.
(38) Franklin, A. D.; Janes, D. B.; Claussen, J. C.; Fisher, T. S.; Sands, T. D. *Appl. Phys. Lett.* **2008**, *92*, 013122.
(39) Ding, S. J.; Chang, B. W.; Wu, C. C.; Lai, M. F.; Chang, H. C. *Anal. Chim. Acta* **2005**, *554*, 43.
(40) Bain, C. D.; Evall, J.; Whitesides, G. M. *J. Am. Chem. Soc.* **1989**, *111*, 7155.
(41) Liu, Y. Y.; Zhu, Y. C.; Zeng, Y.; Xu, F. F. *Nanoscale Res. Lett.* **2009**, *4*, 210.

(42) Cherevko, S.; Chung, C. H. *Sens. Actuators, B* **2009**, *142*, 216.
(43) Mena, M. L.; Yáñez-Sedeño, P.; Pingarrón, J. M. *Anal. Biochem.* **2005**, *336*, 20.
(44) Delvaux, M.; Walcarius, A.; Demoustier-Champagne, S. *Biosens. Bioelectron.* **2005**, *20*, 1587.
(45) Li, Y.; Song, Y. Y.; Yang, C.; Xia, X. H. *Electrochem. Commun.* **2007**, *9*, 981.
(46) Li, X.; Xu, H.; Wu, Q. *Biotechnol. Bioeng.* **2007**, *98*, 764.
(47) Öhgren, K.; Bengtsson, O.; Gorwa-Grauslund, M. F.; Galbe, M.; Hahn-Hägerdal, B.; Zacchi, G. *J. Biotechnol.* **2006**, *126*, 488.